IIETA International Information and Engineering Technology Association
Advancing the World of Information and Engineering

Annales de Chimie - Science des Matériaux
Vol. 48, No. 3, June, 2024, pp. 377-384
Journal homepage: http://iieta.org/journals/acsm

Mechanical and Vibrational Characterization of Reinforced Composite Rubber/Calcium Carbonate for Compressive Optical Sensor Housing

Hari Pratomo[1,2], Sulistyo[1*], Andi Setiono[2], Bambang Widiyatmoko[2], Reza Abdu Rahman[1,3]

[1] Department of Mechanical Engineering, Diponegoro University, Semarang 50275, Indonesia
[2] Research Center for Photonics, National Research and Innovation Agency, South Tangerang 15315, Indonesia
[3] Department of Mechanical Engineering, Faculty of Engineering, Universitas Pancasila, DKI Jakarta 12640, Indonesia

Corresponding Author Email: sulistyo@lecturer.undip.ac.id

https://doi.org/10.18280/acsm.480309

Received: 9 February 2024
Revised: 28 April 2024
Accepted: 26 May 2024
Available online: 30 June 2024

Keywords:
calcium carbonate, deflection, response time, tensile strength, response time

ABSTRACT

A weigh-in-motion (WIM) sensor is a versatile unit that dynamically monitors the vehicle load, which is suitable for high-mobility traffic. However, the dynamic measurement requires sufficient physical property for the sensor housing in order to maintain the effective reading process and response time. The present work assesses the potential of reinforced silicone rubber as a compressive sensor housing. The reinforcement uses calcium carbonate ($CaCO_3$) and spring wire. The tensile strength of the composite rubber increases up to 56.5% by adding 15 wt% $CaCO_3$. The maximum deflection of the composite is obtained at 12.92 mm at a load of 160 kg, which is higher compared to the rubber (maximum load of 70 kg). The spring within the composite maintains sufficient deflection profile around 180-220 kg, indicating a better mechanical strength. The response time for reinforced composite rubber is less than 200 ms (milliseconds), demonstrating a notable reading performance. Moreover, surface observation through scanning electron microscope (SEM) implies suitable material conformity between rubber and $CaCO_3$, making the proposed method can be taken as a convenient manufacturing method for producing compressive sensor housing.

1. INTRODUCTION

The high global trading in modern society causes a tremendous escalation in the logistic distribution. The optimization of logistic distribution is advantageous, allowing to reduce the operational cost, a better timetable delivery, and reduce the emission from transportation. However, the road infrastructure is severely damaged due to overloaded logistic vehicles. The overloaded vehicle is modified to increase its loading capacity, which causes severe problems in road infrastructure and safety [1]. The responsible authority employs a monitoring control system to overcome the issue. It can be done using static load measurement, which is more accurate. However, the process takes time, which causes long queues and is considered uneconomically. Alternatively, dynamic measurement can be performed while the traffic is on the road using a weigh-in-motion (WIM) sensor. Despite that, it has a lower accuracy due to compressive measurement, which is affected by the road condition and vehicle speed [2].

A significant improvement is achieved for the WIM sensor. The piezoelectric is a typical WIM sensor that is generally used considering its low cost and versatility. However, the environment temperature affects it significantly, reducing its readability during the operation. It is affected by environmental exposure and continuous operation, leading to high wear out and degradation [3-5]. Moreover, the lifetime for piezoelectric is extremely short, taking extra cost for an extensive replacement. Capacitive sensors overcome the drawback of piezoelectric sensors. Unfortunately, it is only suitable for static load measurement [6]. The ideal option is a fiber optic sensor with a better response time, relatively low-cost and versatile [7]. The main challenge for fiber optics is exceptionally fragile and needs an external housing to prevent damage and failure during the operation.

The operation of fiber optic for WIM application causes compressive load from the vehicle. The applied load on the sensor generates deflection, which is used as the reading value. Thus, using fiber optics as a compressive sensor demands an external housing to protect the sensor. The designed housing uses a unique approach based on the strain measurement principle according to fiber Bragg grating (FBG) [8]. Dong et al. [9] used a cement-based housing with a maximum load of 8.0 kN without causing an error in the sensor readability. The load variation on the sensor unit also involves elasticity properties to read the cyclic profile, which is essential for traffic conditions. Furthermore, the load absorbed by the housing should be limited to prevent inaccurate reading measurements on the sensor unit [10]. In addition, Shin et al. [11] using modified strain sensor with zinc oxide for motion monitoring, indicating a high reliable measurement (99%) for the received data. It implies the modification of the sensor component with suitable housing is essential for strain sensor.

The ideal option for using external housing comes from rubber-based material. The rubber housing is considered suitable for the cyclic characteristic as a sensor housing [12]. Zhou et al. [13] developed a rubber-based buffer layer for

seismic application. The rubber's elasticity properties allow the sensor to be protected without experiencing significant failure. Rubber-based housing is also economically favorable, with good tailorability and superior temperature resistance [14]. Wang et al. [15] utilized the elasticity behavior of rubber as displacement sensor for automobile crash evaluation, showing the dimension of rubber affects the obtaining results which makes the determination of its elasticity is crucial for data readability. Nevertheless, continuous reading and loading risks the durability and elasticity of the rubber, which probably leads to inaccuracy for long-term application [16]. Thus, reinforcement can be taken to improve the mechanical properties of rubber.

Reinforced rubber is specifically addressed to improve the mechanical properties and maintain the elasticity of the rubber. Bio-based reinforcement using bamboo and jute fabric is considered a sustainable approach. The tensile strength of reinforced rubber was improved up to 1.975 N/mm^2 [17]. Gong et al. [18] applied reinforced rubber with cord spring. The reinforced rubber with cord spring demonstrates a notable response time less than 0.2 ms (millisecond), which is better than rubber without reinforcement. Luo et al. [19] analyzed the multiaxial load for reinforced rubber/cord springs. It shows that the reinforced rubber/cord spring has better fatigue resistance, making it suitable for high-load operation.

Material modification is intended to improve the functionality of the base material [20-22]. In this case, the rubber-based structure has low tensile and hardness properties, which makes reinforcement on the rubber structure also required. Calcium carbonate ($CaCO_3$) can be used as suitable reinforcement for rubber-based material [23]. Gobetti et al. [24] added 10 wt% $CaCO_3$ for butadiene rubber and reported an increment in compressive strength up to 5.9 MPa. Ritonga et al. [25] used $CaCO_3$ (4 wt%) for natural rubber and indicated the same profile where the composite has a better mechanical strength. The calcium carbonate ($CaCO_3$) is also ideal for improving the compressive strength of pavement [26]. Thus, $CaCO_3$ can be considered the ideal candidate to improve the mechanical properties of rubber as compressive sensor housing.

The combined rubber reinforcement (using spring and calcium carbonate) is considered as a proper solution to producing a compressive fiber optic sensor housing. However, the combined approach is rarely discussed in the literature, particularly for high load and cyclic applications such as WIM. Thus, the present work is intended to provide a preliminary study for mechanical and vibrational characterization of the developed rubber structure, including response time, which is essential for compressive sensor application. The preliminary work provides an essential basis for researchers and practitioners to manufacture sensor housing with suitable mechanical properties and response time as compressive sensors housing.

2. MATERIALS AND METHOD

2.1 Sample preparation

The present work used the RTV silicone rubber, considering its high feasibility and producibility for sensor housing as suggested here [27]. To improve the curing time and coagulation of rubber, a catalyst (organic peroxides) was added with four variations: 0.5, 1, 1.5, and 2 wt%. Calcium carbonate ($CaCO_3$) was added for the suitable ratio of silicone rubber. The variation of $CaCO_3$ was set between 0–15 wt% (interval 5 wt%). The composite rubber/$CaCO_3$ was mixed using an agitator mixer at a stirring speed of 1000 rpm for two minutes. Then, the catalyst was added to the mixture to accelerate the polymerization process. The final composition was stirred for one minute. In addition, a vacuum pump was used to evacuate the air within the composite. The evacuation was performed for three minutes.

2.2 Manufacturing the sensor housing

Figure 1a shows the molding construction. It was produced using a 3D printing machine with polylactic acid (PLA) material (Shenzhen Esun Industrial Co., Ltd - China). The housing molding was created in a cylindrical shape (diameter of 25 mm, thickness of 2 mm, and length of 104 mm). A small channel was grooved to place the fiber optic on the outer surface.

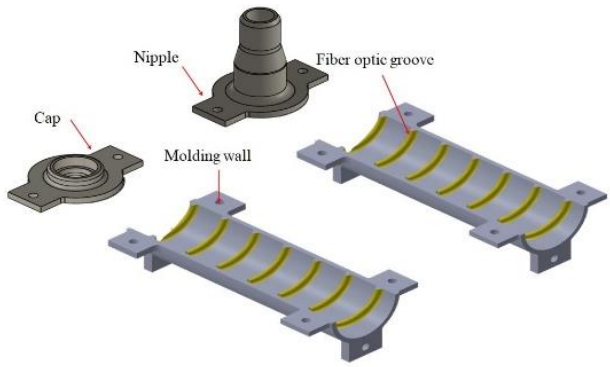

(a) Molding structure to mold composite rubber

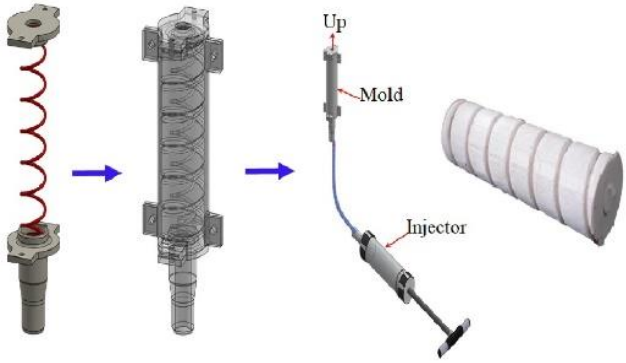

(b) the manufacturing process for producing rubber-based sensor housing

Figure 1. Schematic for production of rubber-based sensor housing

The manufacturing process for producing fiber optic sensor housing is shown in Figure 1b. The process was done using the injection method. Before the injection process, a spiral spring wire with a diameter of 15 mm and a length of 100 mm was placed in the center part of the molding case. Afterward, the silicon gun injected the silicon rubber composite into the molding case from the bottom side. The molding result was then released after 24 hours of curing time.

2.3 Characterization and evaluation

The first characterization evaluated the suitable ratio between silicone rubber and catalyst. It was done by

measuring the viscosity through the falling ball method. The curing time is essential for rubber-based product since it affects the quality and duration for producing the component [28]. Thus, the produced mixtures were investigated under standard-temperature-pressure (STP) conditions to evaluate its curing and coagulation time. The mechanical properties of the produced sample were important to ensure the suitability of the applied force during the measurement [29]. In this work, tensile strength (ASTM D 412) of the composite rubber was measured using a universal testing machine (UTM: Shimadzu AGS 10 kN) at a speed of 500 mm/minute with a grip distance of 85 mm. The hardness test was performed according to ASTM 2240.

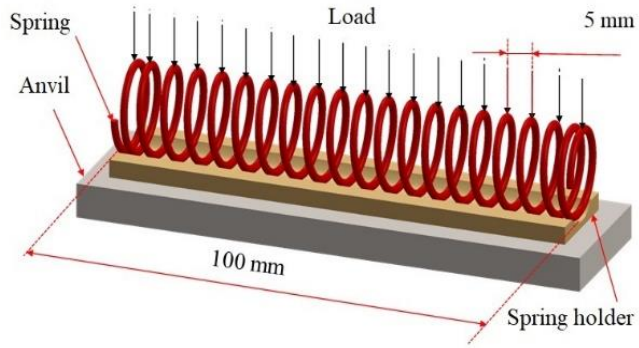

(a) Illustration of load exposure that compresses the employed spiral spring wire

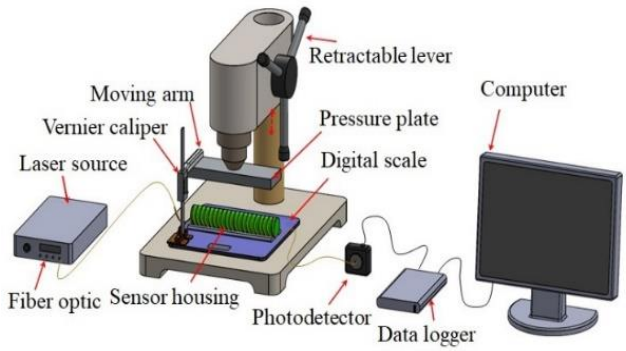

(b) Experiment setup for recovery time measurement

Figure 2. Schematic of the specimen and experimental evaluation of the produced sensor

The composite rubber was reinforced using a spiral spring. The spring was made of steel wire with a tensile strength of 1515 MPa and elongation of 5.16%. The wire diameter is 1 mm with 20 total turns (Figure 2a). Further observation of the steel wire was conducted using Optical Emission Spectroscopy (OES). It was found that the chemical composition of steel spring is: 0.099% Carbon (C), 0.033% Silicon (Si), 0.17% Manganese (Mn), 0.02% Phosphorus (P), 0.0011% Sulfur (S), 0.022% Chromium (Cr), <0.001% Molybdenum (Mo), and 0.001% Nickel (Ni).

Figure 2b displays the recovery time measurement system. Before performing measurement, initial calibration was done by setting the operation parameter to obtain suitable and reliable result from the measurement [30]. The process was repeated several until the obtained result indicating good conformability between the applied force and displacement of the specimen. In this work, the applied load ranged between 10 kg-100 kg with an interval of 10 kg considering the sample size as we presented in Figure 2a. The force acting on the sensor's surface was applied gently to ensure its center position. The employed fiber optic was sourced from a laser diode (λ = 1330 nm) as the input and connected to a photodetector at the output source. The data logger recorded the output voltage from the photodetector. The recovery time was estimated according to the deviation between voltage drop response (t_{drop}) and voltage recovery ($t_{recovery}$) after the load induced onto the sensor.

3. RESULTS AND DISCUSSION

The injection process highly depends on the viscosity of the raw material. Thus, an initial assessment was performed for the RTV with catalyst. As seen in Figure 3, the viscosity, coagulation and curing time indicate an identic pattern. Adding 0.5 wt% catalyst led to the highest viscosity (1.66). It also has the longest duration for coagulation (5 hours) and curing time (more than 120 hours), which is time-consuming and unfavorable for the injection process. Contrary to that, the viscosity of the silicon rubber falls significantly with a catalyst ratio 1.5 wt%. The viscosity decreases by around 17.5%, while the coagulation and curing can be reduced by more than 90%. The profile implies that the higher catalyst content causes rapid solidification of rubber, which can be a catastrophe for the injection process. Thus, the suitable catalyst ratio is 1 wt%, which decreases slightly the viscosity and maintains sufficient time for the injection process.

The mechanical properties of the silicon rubber with $CaCO_3$ are presented in Figure 4. It clearly indicates the influence of $CaCO_3$ on the improvement of the physical properties of the silicon rubber. The hardness level of rubber with $CaCO_3$ elevates around 33.5%-56.5%, which also increases the tensile strength of the rubber matrix. The addition of 5 wt% $CaCO_3$ promotes a higher tensile strength by more than 36.4%. It demonstrates that the physical properties of rubber are suitable for use as sensor housing that experiences mechanical load during the operation. Despite that, the hardness and tensile strength improvement is followed by the decrement on strain break which makes the rubber matrix stiff.

Figure 5 displays the surface observation for rubber with and without $CaCO_3$. The lower $CaCO_3$ causes particle dispersion on the rubber surface (red square in Figure 5b). Local agglomeration is found for a higher $CaCO_3$ content. It can be seen notably in Figure 5c (green square). The rubber's solidification process can affect the dispersion of $CaCO_3$ particles, which probably leads to local agglomeration. It also influences the diffusion of $CaCO_3$ particles into the silicone matrix (red circle in Figure 5b and Figure 5d). It explains the physical changes of the composite rubber, which experiences a better mechanical strength compared to silicon rubber (Figure 4).

Reinforcement for the produced composite rubber is done using spring wire. Thus, the initial deflection characteristic of spring is evaluated in the first place. The deflection profile for the single spring is shown in Figure 6a. It shows the maximum non-linear deflection is 0.57 mm under 40 kg load. Above this region, increasing the load leads to a linear profile corresponding to the deflection rate of 0.04 mm. The plastic region occurs above 230 kg. It shows the average deflection above 0.05 mm. According to the profile, the spring characteristic is suitable as a reinforcement for the composite rubber.

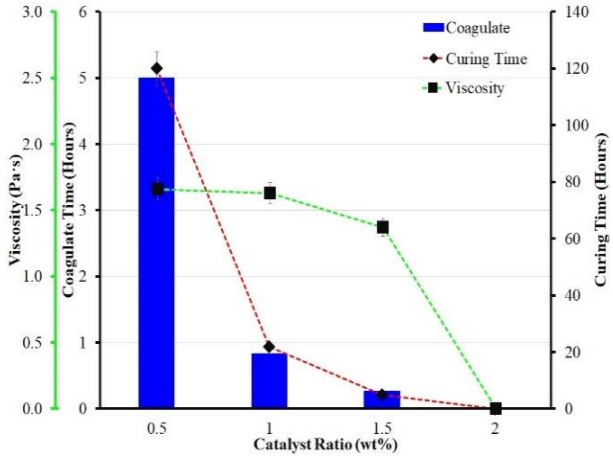

Figure 3. The effect of catalyst on viscosity, coagulation and curing time for the silicone rubber

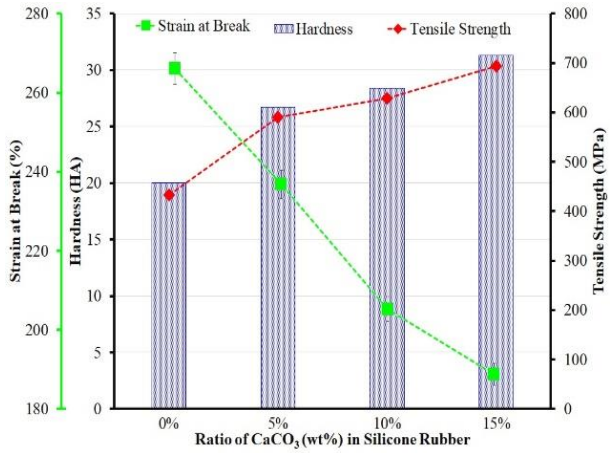

Figure 4. The changes in mechanical strength for silicone rubber with $CaCO_3$

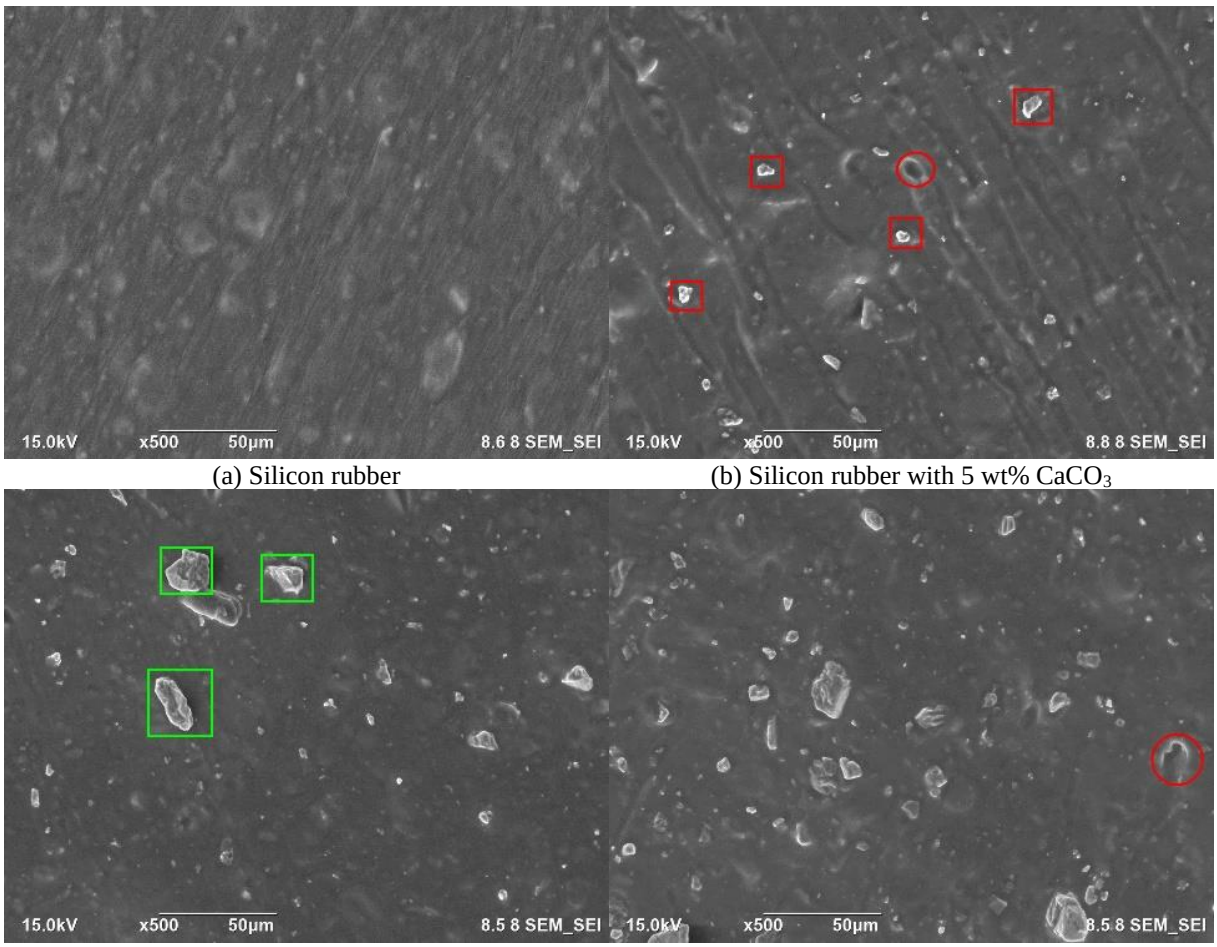

(a) Silicon rubber (b) Silicon rubber with 5 wt% $CaCO_3$

(c) Silicon rubber with 10 wt% $CaCO_3$ (d) Silicon rubber with 15 wt% $CaCO_3$

Figure 5. Surface observation of silicon rubber and its composites

The effect of the $CaCO_3$ ratio for the composite rubber can be observed distinctively in Figure 6b. The maximum load for the silicon rubber is only 70 kg, with a maximum deflection of 13.54 mm. Contrary to that, adding $CaCO_3$ promotes a better physical structure of the rubber, allowing it to handle a higher load. Using 5 wt% $CaCO_3$ increases the maximum load for the rubber above 40%. As a result, it makes the rubber advantageous as a compressive sensor housing. The maximum deflection for the composite rubber is only slightly lower than the silicone rubber (less than 5%). Thus, the addition of $CaCO_3$ at the given ratio maintains the elasticity profile of the rubber while at the same time improving its maximum load capacity.

Reinforcement of the rubber using spring can be seen notably in Figure 6c, particularly for the silicon rubber. The maximum load for the reinforced silicon rubber increased more than twice times. It makes silicon rubber able to handle a more significant compressive force.

Despite that, the effect of $CaCO_3$ on the reinforced rubber varies. The highest increment for the reinforced rubber is obtained by composite rubber with 10 wt% $CaCO_3$, which increases around 84.6%. At a higher ratio (15 wt% $CaCO_3$), the maximum load is only increased by 12.5%. It confirms the SEM profile (Figure 5d), which indicates particle diffusion within the rubber matrix.

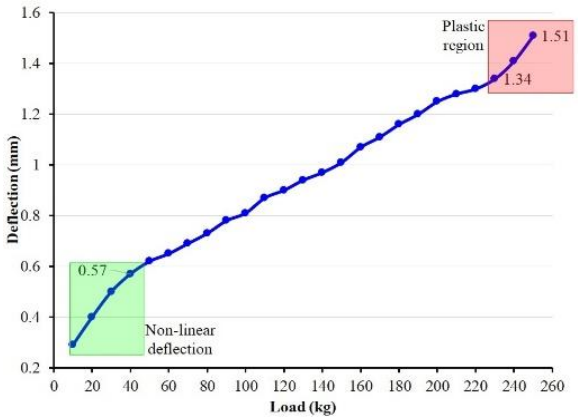

(a) Single spring

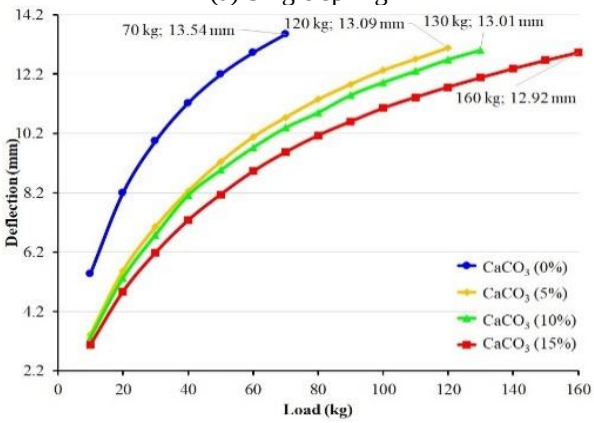

(b) Composite rubbers

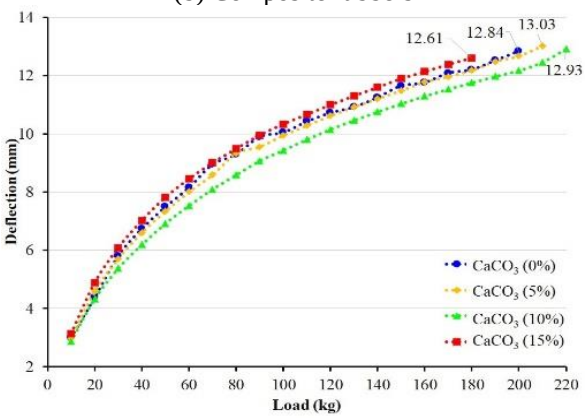

(c) Reinforced composite rubbers with spring

Figure 6. Deflection profile

The response time profile for silicone rubber demonstrates a slight variation under a small load (less than 60 kg, Figure 7a) with an average response time of 140 ms. However, the response time increases rapidly at 70 kg. It corresponds to the maximum deflection of the silicone rubber (Figure 6a). The response time profile changes variably for the composite rubber. It is affected by the strain effect which generally related to the uniaxial compression load [31], similar with the actual application of WIM sensor which experiences continuous load from the vehicle. According to the measurement result in this work, the composite with 5 wt% has a stable response between 30–70 kg, while the initial and ending profile indicate a shallow profile, which correspond to a faster response time (Figure 7b). The higher $CaCO_3$ contents (Figure 7c and Figure 7d) demonstrate a fluctuate which is affected by its low elasticity (Figure 4). It strengthens the key properties for the sensor housing to accommodate various load application and distribute it to the fiber optic.

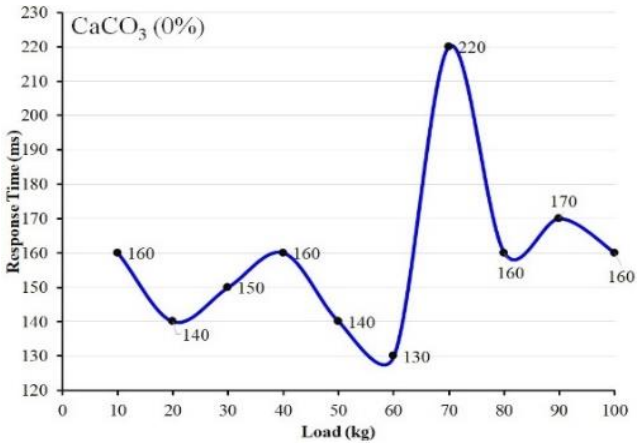

(a) Silicon rubber without $CaCO_3$

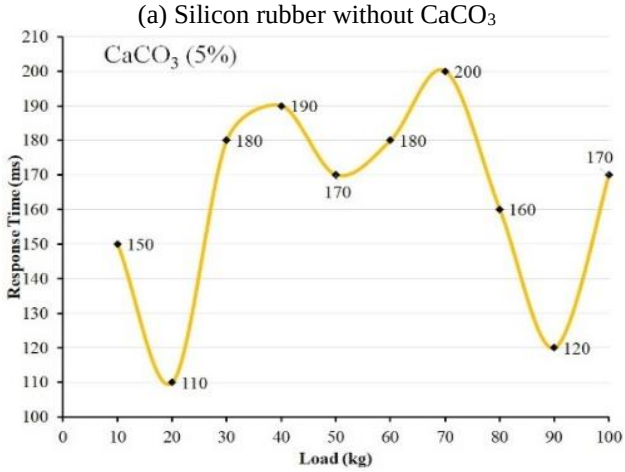

(b) Silicon rubber with 5 wt% $CaCO_3$

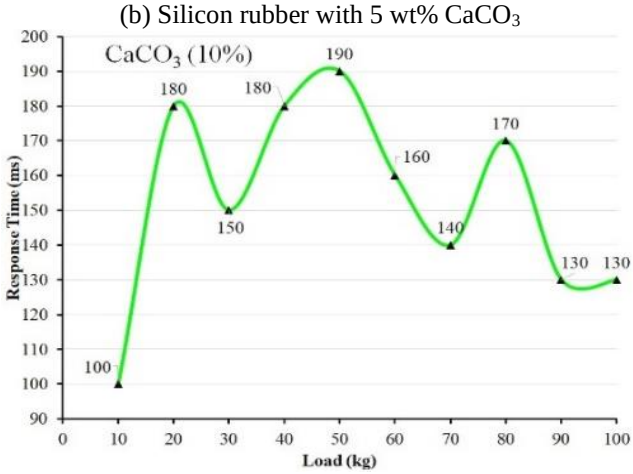

(c) Silicon rubber with 10 wt% $CaCO_3$

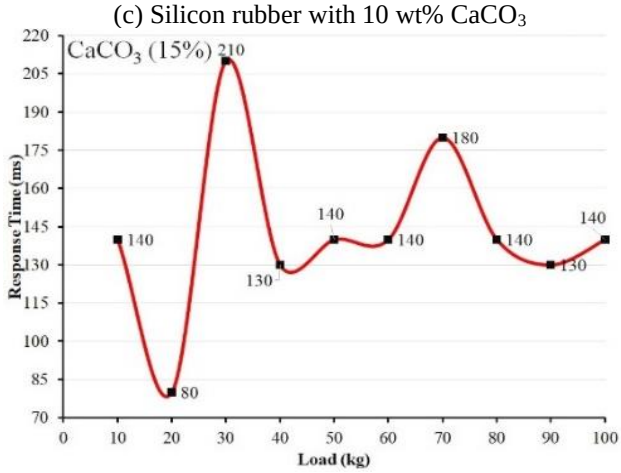

(d) Silicon rubber with 15 wt% $CaCO_3$

Figure 7. The response time profile for the silicon rubber without reinforcement

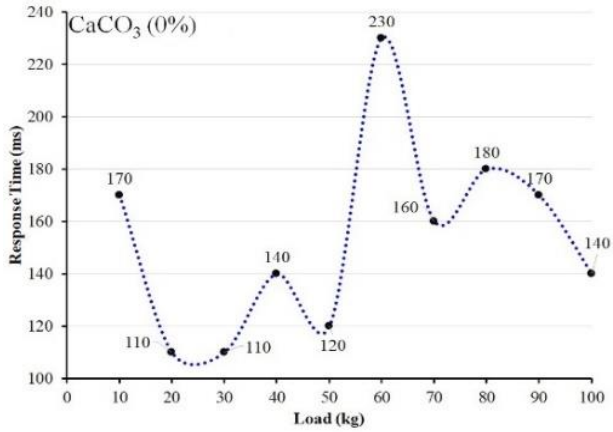

(a) Reinforced silicon rubber without $CaCO_3$

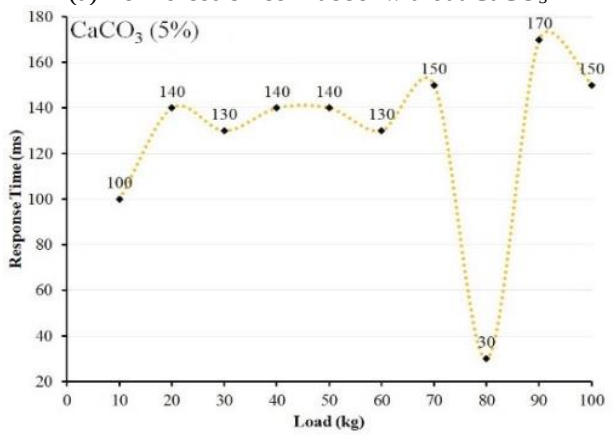

(b) Reinforced silicon rubber with 5 wt% $CaCO_3$

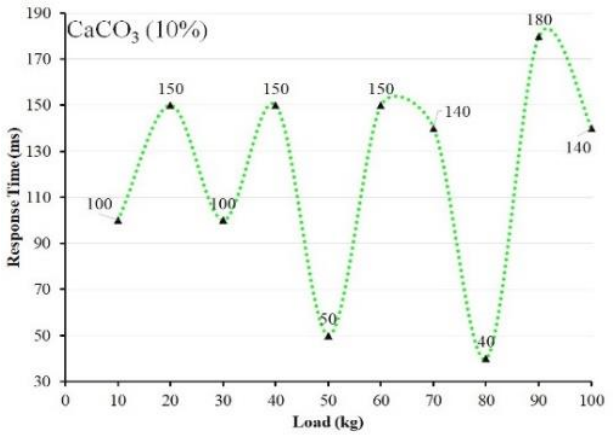

(c) Reinforced silicon rubber with 10 wt% $CaCO_3$

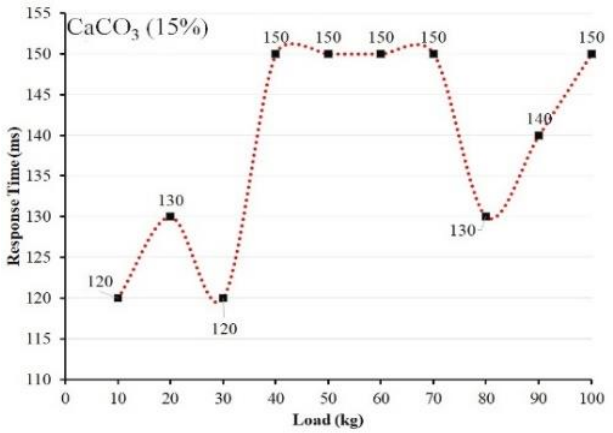

(d) Reinforced silicon rubber with 15 wt% $CaCO_3$

Figure 8. The response time profile for the reinforced silicon rubber

The peak response time for reinforced silicone rubber occurs at a lower load (60 kg, Figure 8a). It can be seen as a drawback for the rubber, which experiences a slower response time at a lower load. The slower response time generally linked to uneven redistribution of strain, which also affected by the mechanical properties of the housing [32]. The reinforced composite rubber with 5 wt% $CaCO_3$ (Figure 8b) demonstrates a stable response time under 70 kg, which can have a positive impact. The response times became faster at 80 kg and increased at higher loads (90 kg and 100 kg). It makes the fluctuation occur at a sufficient load. Figure 8c indicates a significant change for the reinforced composite rubber with 10 wt%. It becomes more fluctuate, severely damaging the data reading for the applied sensor. One unique profile is shown for the reinforced silicone rubber with 15 wt% $CaCO_3$ (Figure 8d). It has a faster response time with a lower load (10-30 kg), and then becomes slower at steady results with the applied load between 40-70 kg. It experiences a slight increment in the response time (130 ms with 80 kg load), and consistently increases as the load becomes higher.

To understand the impact of reinforcement for the silicon rubber housing, Figure 9 plots the average response time for each model. One can be observed the reinforced silicon rubber has a lower average of response time, with the lowest value is obtained using 10 wt% $CaCO_3$. The lower variation on the response time is desirable, particularly for dynamic measurement [33] since the signal can be generated sufficiently with minimum deviation on the reading results. It signifies the key advantages for using reinforced sensor housing for dynamic measurement. Moreover, the addition of 5 wt% and 10 wt% of $CaCO_3$ can be taken as the suitable ratio, since each composition has the lowest average of response time while adding more $CaCO_3$ (15 wt%) causing a higher response time for the reinforced sensor housing. It demonstrates the addition of $CaCO_3$ and suitable wire diameter are essential to obtain a reliable structure of the housing.

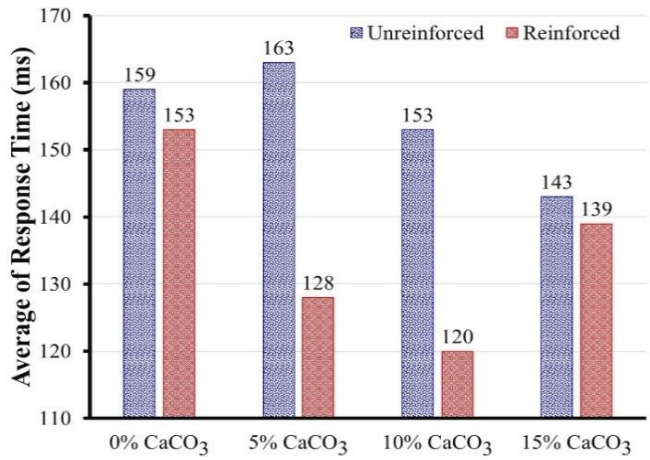

Figure 9. The average response time of the evaluated rubber-based sensor housing

4. CONCLUSION

The mechanical and vibrational properties of rubber-based sensor housing are improved using calcium carbonate ($CaCO_3$) and spring wire. The composite rubber with $CaCO_3$ indicates a substantial increment of tensile strength up to 693.4 MPa using 15 wt% $CaCO_3$. The same composite also has a better

hardness level (31.3) strain at break 188.8%. It implies that the elasticity of the composite is still sufficient to accommodate the vibrational motion as compressive sensor housing. The maximum load for the composite can be improved more than twice, with the lowest deflection of 12.92 mm. Adding spring within the composite structure promotes a higher load capability with a maximum load of 220 kg. The change in mechanical structure for the composite rubber minimizes the slow response time. The average response time for composite rubber is less than 200 ms, with the lowest value is 120 ms obtained by reinforced rubber.

The study indicates the suitability of the produced sensor housing for dynamic WIM measurement. However, the study is limited to maximum load of 100 kg for evaluation the response time, which can be further assessed at higher load. Moreover, it is advisable to evaluate the effect of environmental exposure on the readability of the measurement under actual dynamic load. It can be taken for future work to obtain the most advance compressive sensor housing for WIM applications.

ACKNOWLEDGMENT

The authors gratefully acknowledge the support and provision of laboratory facilities by the National Research and Innovation Agency (Badan Riset dan Inovasi Nasional/BRIN) and Universitas Diponegoro. This project has been funded by Indonesia Endowment Fund for Education Agency (LPDP) through the RIIM-BRIN program, with reference number 37/II.7/HK/2023.

REFERENCES

[1] Klinjun, N., Kelly, M., Praditsathaporn, C., Petsirasan, R. (2021). Identification of factors affecting road traffic injuries incidence and severity in Southern Thailand based on accident investigation reports. Sustainability, 13(22): 12467. https://doi.org/10.3390/su132212467

[2] Zhang, L., Cheng, X., Wu, G. (2021). A bridge weigh-in-motion method of motorway bridges considering random traffic flow based on long-gauge fibre Bragg grating sensors. Measurement, 186: 110081. https://doi.org/10.1016/j.measurement.2021.110081

[3] Guan, M., Liu, Y., Du, H., Long, Y., An, X., Liu, H., Cheng, B. (2023). Durable, breathable, sweat-resistant, and degradable flexible sensors for human motion detection. Chemical Engineering Journal, 462: 142151. https://doi.org/10.1016/j.cej.2023.142151

[4] Suyitno, B.M., Rahman, R.A., Sukma, H., Rahmalina, D. (2022). The assessment of reflector material durability for concentrated solar power based on environment exposure and accelerated aging test. Eastern-European Journal of Enterprise Technologies, 6(12): 120. https://doi.org/10.15587/1729-4061.2022.265678

[5] Yang, X., Wang, X., Podolsky, J., Huang, Y., Lu, P. (2024). Addressing wander effect in vehicle weight monitoring: An advanced hybrid weigh-in-motion system integrating computer vision and in-pavement sensors. Measurement, 234: 114870. https://doi.org/10.1016/j.measurement.2024.114870

[6] Sroka, R., Burnos, P., Gajda, J. (2019). Vehicle's axle load sensors in weigh-in-motion systems. In Physical and Chemical Sensors: Design, Applications & Networks (Book Series: Advances in Sensors: Reviews, Vol. 7), International Frequency Sensor Association (IFSA) Publishing, Barcelona, pp. 49-67.

[7] Wang, J., Han, Y., Cao, Z., Xu, X., Zhang, J., Xiao, F. (2023). Applications of optical fiber sensor in pavement Engineering: A review. Construction and Building Materials, 400: 132713. https://doi.org/10.1016/j.conbuildmat.2023.132713

[8] Alamandala, S., Prasad, R.S., Pancharathi, R.K., Pavan, V.D.R., Kishore, P. (2021). Study on bridge weigh in motion (BWIM) system for measuring the vehicle parameters based on strain measurement using FBG sensors. Optical Fiber Technology, 61: 102440. https://doi.org/10.1016/j.yofte.2020.102440

[9] Dong, W., Li, W., Guo, Y., Sun, Z., Qu, F., Liang, R., Shah, S.P. (2022). Application of intrinsic self-sensing cement-based sensor for traffic detection of human motion and vehicle speed. Construction and Building Materials, 355: 129130. https://doi.org/10.1016/j.conbuildmat.2022.129130

[10] Masud, M.M., Haider, S.W. (2023). Effect of static weight errors on Weigh-in-Motion (WIM) system accuracy. Measurement, 206: 112301. https://doi.org/10.1016/j.measurement.2022.112301

[11] Shin, D., Kim, E., Woo, G., Kim, T. (2023). Stretchable optical fiber strain sensor comprising zinc oxide and PDMS for human motion monitoring. Journal of Mechanical Science and Technology, 37(6): 3205-3212. https://doi.org/10.1007/s12206-023-0544-0

[12] Sujon, M., Dai, F. (2021). Application of weigh-in-motion technologies for pavement and bridge response monitoring: State-of-the-art review. Automation in Construction, 130: 103844. https://doi.org/10.1016/j.autcon.2021.103844

[13] Zhou, T., He, T., Wei, Y., Li, S. (2023). Seismic design and performance analysis of perforated rubber buffer layer in tunnel. Structures, 57(2023): 105069. https://doi.org/10.1016/j.istruc.2023.105069

[14] Dudziński, P.A., Chołodowski, J. (2021). A method for predicting the internal motion resistance of rubber-tracked undercarriages, Pt. 1. A review of the state-of-the-art methods for modeling the internal resistance of tracked vehicles. Journal of Terramechanics, 96: 81-100. https://doi.org/10.1016/j.jterra.2021.02.006

[15] Wang, Y.Y., Yang, J.B., Qian, J.B., Hou, H.P., Yan, H.J., Zhu, T.Y., Chen, J., Wang, R.M., Jin, M.S. (2022). A novel high-performance draw-wire displacement sensor for automobile crash test. Instruments and Experimental Techniques, 65(1): 142-151. https://doi.org/10.1134/S0020441222010134

[16] Brzozowski, K., Maczyński, A., Ryguła, A., Konior, T. (2023). A weigh-in-motion system with automatic data reliability estimation. Measurement, 221: 113494. https://doi.org/10.1016/j.measurement.2023.113494

[17] Razdan, S., Marathe, D.S. (2023). Uniaxial tensile properties for bamboo and jute fabric reinforced natural rubber. Materials Today: Proceedings, 80: 591-596. https://doi.org/10.1016/j.matpr.2022.11.053

[18] Gong, S., Oberst, S., Wang, X. (2020). An experimentally validated rubber shear spring model for vibrating flip-flow screens. Mechanical Systems and Signal Processing, 139: 106619. https://doi.org/10.1016/j.ymssp.2020.106619

[19] Luo, G., Guo, J., Zhang, C., Yang, X. (2023). Life prediction of cord/rubber laminates under multiaxial fatigue. International Journal of Fatigue, 174: 107733. https://doi.org/10.1016/j.ijfatigue.2023.107733.
[20] Suyitno, B.M., Anggrainy, R., Plamonia, N., Rahman, R.A. (2023). Preliminary characterization and thermal evaluation of a direct contact cascaded immiscible inorganic salt/high-density polyethylene as moderate temperature heat storage material. Results in Materials, 19: 100443. https://doi.org/10.1016/j.rinma.2023.100443
[21] Widiyatmoko, B., Rofianingrum, M.Y., Hanto, D., Prakosa, J.A., Mulyanto, I., Ula, R.K., Bayuwati, D., Setiono, A. (2022). Macrobending loss in wrapped fiber optic for load detections. Applied Optics, 61(13): 3786-3792. https://doi.org/10.1364/ao.451825
[22] Adji, R.B., Rahman, R.A. (2023). Increasing the feasibility and storage property of cellulose-based biomass by forming shape-stabilized briquette with hydrophobic compound. Case Studies in Chemical and Environmental Engineering, 8: 100443. https://doi.org/10.1016/j.cscee.2023.100443
[23] Fang, Q., Song, B., Tee, T.T., Sin, L.T., Hui, D., Bee, S.T. (2014). Investigation of dynamic characteristics of nano-size calcium carbonate added in natural rubber vulcanizate. Composites Part B: Engineering, 60: 561-567. https://doi.org/10.1016/j.compositesb.2014.01.010
[24] Gobetti, A., Cornacchia, G., Gelfi, M., Ramorino, G. (2023). White steel slag from ladle furnace as calcium carbonate replacement for nitrile butadiene rubber: A possible industrial symbiosis. Results in Engineering, 18: 101229. https://doi.org/10.1016/j.rineng.2023.101229
[25] Ritonga, A.H., Jamarun, N., Arief, S., Aziz, H., Tanjung, D.A., Isfa, B., Sisca, V., Faisal, H. (2022). Organic modification of precipitated calcium carbonate nanoparticles as filler in LLDPE/CNR blends with the presence of coupling agents: Impact strength, thermal, and morphology. Journal of Materials Research and Technology, 17: 2326-2332. https://doi.org/10.1016/j.jmrt.2022.01.125
[26] Yildizel, S.A., Tayeh, B.A., Uzun, M. (2022). The evaluation of calcium carbonate added and basalt fiber reinforced roller compacted high performance concrete for pavement. Case Studies in Construction Materials, 17: e01293. https://doi.org/10.1016/j.cscm.2022.e01293
[27] El-Khatib, A.M., Elesh, E., Hamada, M.S., Sabry, E.M., Gouda, M.M. (2024). Study attenuation parameters and physical properties of silicone rubber reinforced with nano- and micro-sized aluminum oxide composites. Silicon, 1-14. https://doi.org/10.1007/s12633-024-02847-7
[28] Unruan, M., Unruan, S., Pisitpipathsin, N., Yimnirun, R. (2021). Curing characteristics exploration of rubber compound by using capacitance sensor. Journal of Polymer Research, 28: 1-6. https://doi.org/10.1007/s10965-021-02835-0
[29] Hiremath, S., Kim, T.W. (2024). Detection of physical signal and time-frequency analysis owing to the impact on rubber material using a piezoelectric sensor. Journal of Mechanical Science and Technology, 38: 2455–2463. https://doi.org/10.1007/s12206-024-0424-2
[30] Chen, G., Liu, H., Gao, R. (2023). Calibration technology of optical fiber strain sensor. Journal of Shanghai Jiaotong University (Science), 28(5): 551-559. https://doi.org/10.1007/s12204-022-2406-9
[31] Lin, S.Q., Tan, D.Y., Yin, J.H., Li, H. (2021). A novel approach to surface strain measurement for cylindrical rock specimens under uniaxial compression using distributed fibre optic sensor technology. Rock Mechanics and Rock Engineering, 54: 6605-6619. https://doi.org/10.1007/s00603-021-02648-z
[32] Zhao, L., Tang, F., Li, G., Li, H.N. (2024). Crack width measurement with OFDR distributed fiber optic sensors considering strain redistribution after structure cracking. Journal of Civil Structural Health Monitoring, 14(4): 1091-1109. https://doi.org/10.1007/s13349-024-00777-x
[33] Wright, D.N., Züchner, M., Annavini, E., Escalona, M.J., Hammerlund Teige, L., Whist Tvedt, L.G., Lervik, A., Haga, H.A., Guiho, T., Clausen, I., Glott, T., Boulland, J.L. (2024). From wires to waves, a novel sensor system for in vivo pressure monitoring. Scientific Reports, 14(1): 7570. https://doi.org/10.1038/s41598-024-58019-5